Thermodynamic stability of hydrogen hydrates of ice I_c and II structures

Lukman Hakim, Kenichiro Koga, and Hideki Tanaka
Department of Chemistry, Faculty of Science, Okayama University, 3-1-1 Tsushima, Kitaku, Okayama 700-8530, Japan
(Received 6 August 2010; published 13 October 2010)

The occupancy of hydrogen inside the voids of ice I_c and ice II, which gives two stable hydrogen hydrate compounds at high pressure and temperature, has been examined using a hybrid grand-canonical Monte Carlo simulation in wide ranges of pressure and temperature. The simulation reproduces the maximum hydrogen-to-water molar ratio and gives a detailed description on the hydrogen influence toward the stability of ice structures. A simple theoretical model, which reproduces the simulation results, provides a global phase diagram of two-component system in which the phase transitions between various phases can be predicted as a function of pressure, temperature, and chemical composition. A relevant thermodynamic potential and statistical-mechanical ensemble to describe the filled-ice compounds are discussed, from which one can derive two important properties of hydrogen hydrate compounds: the isothermal compressibility and the quantification of thermodynamic stability in term of the chemical potential.

DOI: 10.1103/PhysRevB.82.144105 PACS number(s): 64.70.Ja

I. INTRODUCTION

Storage of hydrogen has been actively investigated to meet the demand on environmentally clean and efficient hydrogen-based fuel.[1] A search for practical hydrogen-storage materials leads to an intensive exploration of host-guest compounds consisting of simple molecules.[2–5] It has long been believed that hydrogen is too small to stabilize the hydrate cages, and therefore cannot form hydrates by itself. However, synthesis of the hydrogen clathrate hydrate of structure II (Ref. 6) and structure H,[7] as confirmed later by a theoretical calculation,[8,9] implies that hydrogen molecules, despite of their small size as guest species, can stabilize a variety of host lattices of water by means of single and multiple occupancies. Hydrogen hydrate is considered as a potential candidate for hydrogen storage, which is particularly interesting in industry, and its unique features have stimulated scientific curiosity in general.

It has also been reported that hydrogen molecules can be engaged in the interstitial spaces of ice II and cubic ice (I_c), giving two stable hydrate compounds, or filled ices, called C_1 and C_2.[10] The water lattice in C_1 consists of hydrogen-bonded water hexagonal rings stacked along c axis, thus provides hollow cylindrical spaces, in the same manner as ice II.[11] The diameter of those cylindrical spaces is sufficient to accommodate hydrogen molecules. In such sense, C_1 can be viewed as ice II filled with hydrogen molecules. Light noble gases such as helium[12] and neon[13] are also known to form hydrates of ice II structure. On the other hand, the water lattice of C_2 is a diamondlike structure equivalent to ice I_c structure,[11] and thus it can be viewed as ice I_c where its interstitial spaces are occupied by hydrogen. The C_2 is a hydrogen-rich crystalline compound with 1:1 molar ratio of water-to-hydrogen, corresponds to 110 g L^{-1} hydrogen, and it is stable down to 500 MPa at 77 K.[6]

Given the variety of hydrogen hydrates, it is of fundamental importance that the stability and the phase behavior of a water-hydrogen system are systematically studied in the pressure p, temperature T, and chemical-composition space. Unfortunately, the thermodynamic stability of C_1 and C_2 relative to other water-hydrogen composite phases in a wide range of thermodynamic conditions has been scarcely explored. On the other hand, constructing a global phase diagram is a tedious task from experimental view point, considering the number of thermodynamic states to be explored. It is even more difficult to carry out experiments for C_2 in high pressure of gigapascal order.

Here we present complementary study on hydrogen occupancy inside ice II and ice I_c; a Monte Carlo (MC) simulation that reproduces experimental observations and a simple theoretical calculation that provides a global phase behavior for realistic models of C_1 and C_2. We first examine the ensembles and the relevant thermodynamic potentials to describe clathrate hydrate compounds. A statistical mechanical theory by van der Waals and Platteeuw (vdWP) is modified to treat a condition where the volume, V, is significantly dependent on the pressure. On the basis of this statistical mechanical theory along with MC simulations, the thermodynamic stability of both hydrogen hydrates structures is discussed. The compressibility of various ice forms is also investigated, which turns out to be one of the most intriguing properties. The preliminary results were given in a previous letter.[14]

II. SIMULATION METHOD

A. Intermolecular interaction model and ices structure

In the present study, all molecular interactions are described by the sum of simple site-site pair potential

$$\phi = \sum_{i,j} \left[4\varepsilon_{ij} \left\{ \left(\frac{\sigma_{ij}}{r_{ij}} \right)^{12} - \left(\frac{\sigma_{ij}}{r_{ij}} \right)^{6} \right\} + \frac{Z_i Z_j e^2}{r_{ij}} \right]. \quad (1)$$

Hydrogen molecule is modeled as a linear rigid rotor with a single Lennard-Jones (LJ) potential site and a negative charge site both at the center of mass and two positive charges at the individual protons separated by 0.07414 nm.[15] The water-water interaction is described by TIP4P potential.[16] This potential has often been used in the study of water, and it is believed to be the most reliable within the

TABLE I. Potential parameters for hydrogen and TIP4P water models. In hydrogen model, the negative charge sit at the center of linear rigid rotor. In TIP4P water model, the negative charge sits on a bisector of two OH bonds, denoted as M.

Model	Site	q (e)	σ (0.1 nm)	ε (kJ mol^{-1})
H_2	H	+0.4932		
	Center	−0.9864	3.038	0.2852
TIP4P	H	+0.5200		
	O		3.154	0.6480
	M	−1.0400		

framework of pair potential having a rigid body, at least in reproducing the important properties of pure water and ice.[17] The TIP4P model consists of four interaction sites: a positive charge, q_H on the hydrogen atom, a negative charge $(-2q_H)$ on the bisector of two OH bonds (denoted as M), and an LJ interaction between oxygen atoms. The detailed potential parameters for both models are given in Table I. The interaction between water and hydrogen is described by assuming Lorentz-Berthelot mixing rule

$$\sigma_{12} = \frac{\sigma_1 + \sigma_2}{2}, \tag{2}$$

$$\varepsilon_{12} = \sqrt{\varepsilon_1 \varepsilon_2}. \tag{3}$$

The interaction potentials for all pairs of molecules are truncated smoothly at (r_c=)0.8655 nm (Ref. 18) and discontinuity is avoided by multiplying the potential with a switching function,

$$f_s(r) = \frac{(r - r_c)^3\{10(r - r_l)^2 - 5(r - r_l)(r - r_c) + (r - r_c)^2\}}{(r_l - r_c)^5}, \tag{4}$$

where r is the distance between two centers of mass and r_l is the distance where the switching function begins to take effect with $r_l - r_c = 0.2$ nm. The standard correction for LJ interactions is made by assuming uniform molecular arrangement beyond the truncation distance. The simulation box for ice II structure is taken to be a rectangular prism (a =2.597 nm, b=2.249 nm, and c=2.501 nm) containing 576 water molecules, while that for ice I_c is taken to be a cubic box (a=3.864 nm) containing 1728 water molecules (216 unit cells). The ice I_c configurations are generated according to Bernal-Fowler rules[19] so as to have no net polarization.

B. GC/NPT MC simulation

The accommodation of hydrogen molecules inside ice II (C_1) and ice I_c (C_2), along with their stability under various thermodynamic states, is investigated using a hybrid type of grand-canonical (GC) and isothermal-isobaric (NPT) MC simulations. The accommodation is regarded as an adsorption of the gas in the cavities of ice structures, which can be evaluated as typical adsorption process by GCMC simulation. In this simulation, temperature T and the number of water molecules N_w are kept fixed in the whole process. An insertion or a deletion of hydrogen is attempted with the chemical potential of guest hydrogen (μ_g) and the instantaneous volume fixed. A trial insertion is made at an arbitrary position with randomly chosen polar (θ) and azimuthal (ϕ) angles. The insertion is accepted with the probability

$$P_{\text{insert}} = \min\left\{1, \frac{\exp[\beta(\mu_g' - w)]\sin\theta\ \Lambda^{-3}V}{N_g + 1}\right\}, \tag{5}$$

where w is the interaction energy of the inserted molecule with the surrounding ones. N_g, Λ, and h are the number of guest (hydrogen) molecules, the thermal de Broglie wavelength, and Planck constant, respectively. μ_g' stands for the chemical potential of hydrogen that excludes the contribution from the free rotational motion and β is $1/k_BT$ with Boltzmann constant k_B. Trial deletion of a randomly chosen hydrogen molecule out of N_g is accepted with the probability

$$P_{\text{delete}} = \min\left\{1, \frac{\exp[\beta(-\mu_g' + w)]N_g}{\sin\theta\ \Lambda^{-3}V}\right\}. \tag{6}$$

We assume that the hydrostatic pressure on the hydrate is equal to that of the hydrogen fluid. A relation to the relevant thermodynamic potential is discussed below. The pressure covered in this study is of gigapascal order, which can lead to an alternation of cell dimension. Therefore, to account for this condition, a volume change is attempted according to the standard NPT MC simulation. The pressure p is set to a constant corresponding to the prescribed chemical potential of guest hydrogen and temperature in the rest of the procedures. In this GC/NPT MC simulation, a single step consists of a trial hydrogen molecule insertion or deletion with the same probability, followed by subsequent five trial moves of randomly chosen water or hydrogen molecules and a trial volume change. Each MC simulation is carried out for at least 10^8 steps.

C. NVT MC simulation and chemical potential for hydrogen fluid

The equation of state, which relates the chemical potential of guest fluid with the pressure at particular temperature, is not known for hydrogen fluid interacting with the prescribed potential. The chemical potential of hydrogen fluid with number density ρ at temperature T is given by

$$\mu_g(T,p) = k_BT[\ln\{\rho\Lambda^3\} - 1 + \ln\{h^2/4\pi^2 I k_B T\}] + \int_0^\rho (p - \rho k_B T)/\rho^2 d\rho + p/\rho, \tag{7}$$

where I is the moment of inertia. Here, an NVT MC simulation of hydrogen fluid is carried out in order to establish the relation between the pressures and number density.[8] For this purpose, the number of hydrogen molecules is taken to be in a range of 96–589 molecules so that the system volume falls in a certain range proportional to the volume of ice II and ice I_c. The isotherms are depicted in Fig. 1, where the real hydrogen fluid behaves like an ideal gas with rigid rotors at low

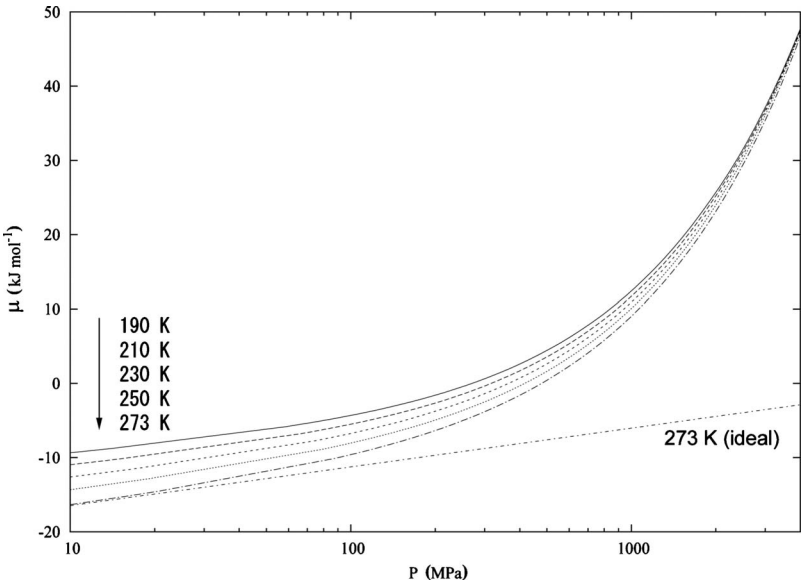

FIG. 1. Pressure and temperature dependence of chemical potential for hydrogen fluid. The linear line shows the chemical potential of hydrogen treated as ideal fluid.

pressure due to its small size and weak attractive interaction. As the pressure increases, the chemical potential significantly deviates from that for the ideal gas due to the strong intermolecular interaction.

III. RESULT AND DISCUSSION

A. Accommodation of hydrogen inside ice I_c and ice II

The representative structures for C_1 and C_2 obtained from GC/NPT MC simulations are given in Fig. 2. In the C_1 structure, it is seen that the cylindrical voids of ice II are filled with hydrogen molecules which align themselves in a quasi-one-dimensional arrangement. In the case of C_2 structure, a hydrogen molecule is located in each interstice of ice I_c. The number of hydrogen molecules encaged is dependent significantly on the applied pressure.

The pressure dependence of hydrogen-to-water molecular ratio in C_1 is shown in Fig. 3(a). The ratio gradually increases as the compression proceeds, which is in sharp contrast to the behavior of common clathrate hydrates where high occupancy is required for the thermodynamic stability of the host structure. This arises from the fact that ice II is a stable ice form even without hydrogen molecules in the region of temperature-pressure plane studied while a usual clathrate is not stable in its empty state. The potential energy arising from the water-water interaction shows no disruption in the pressure range where hydrogen molecules partially occupy the voids of ice II. This also indicates that the structure of C_1 is retained even when the voids of ice II are only partially occupied [Fig. 2(e)]. The encaged hydrogen, however, further enhances the stability of ice II structure and extends its stable region to higher pressure. The highest hydrogen-to-water molecular ratio is found to be 1:6 at all temperatures studied, which is in good agreement with the experimental finding.[10]

In case of C_2, as shown in Fig. 3(b), the hydrogen-to-water molecular ratio rapidly changes in a certain narrow range of pressure and, in particular, it does abruptly in high temperatures. The discontinuity in hydrogen-to-water molecular ratio is also accompanied by a discontinuity in the water-water interaction energy, which further indicates that a

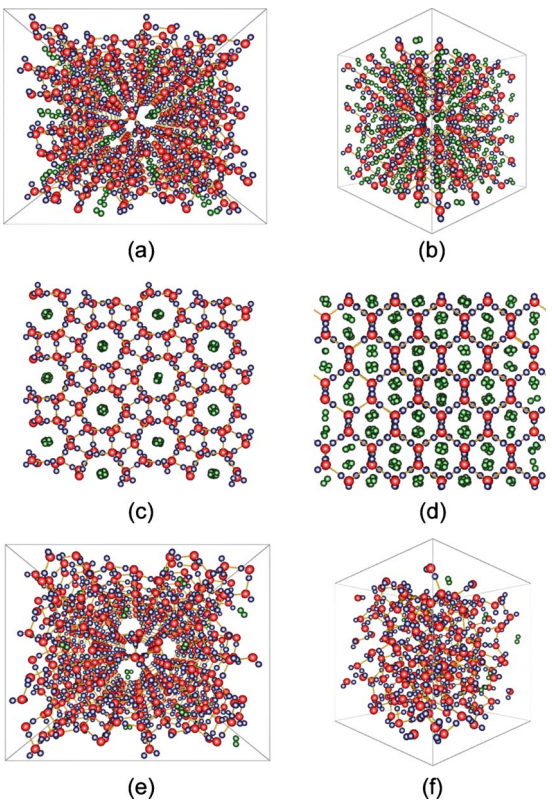

FIG. 2. (Color online) Structures of C_1 and C_2 in various hydrogen occupancy, obtained from GCMC simulation. On the left side: C_1 with maximum hydrogen occupancy (T=273 K, p=2100 MPa) in (a) perspective and (c) orthographic view and (e) C_1 with partial hydrogen occupancy (T=273 K, p=300 MPa). On the right side: C_2 with maximum hydrogen occupancy (T=273 K, p=3500 MPa) in (b) perspective and (d) orthographic view and (f) C_2 with partial hydrogen occupancy (T=273 K, p=700 MPa).

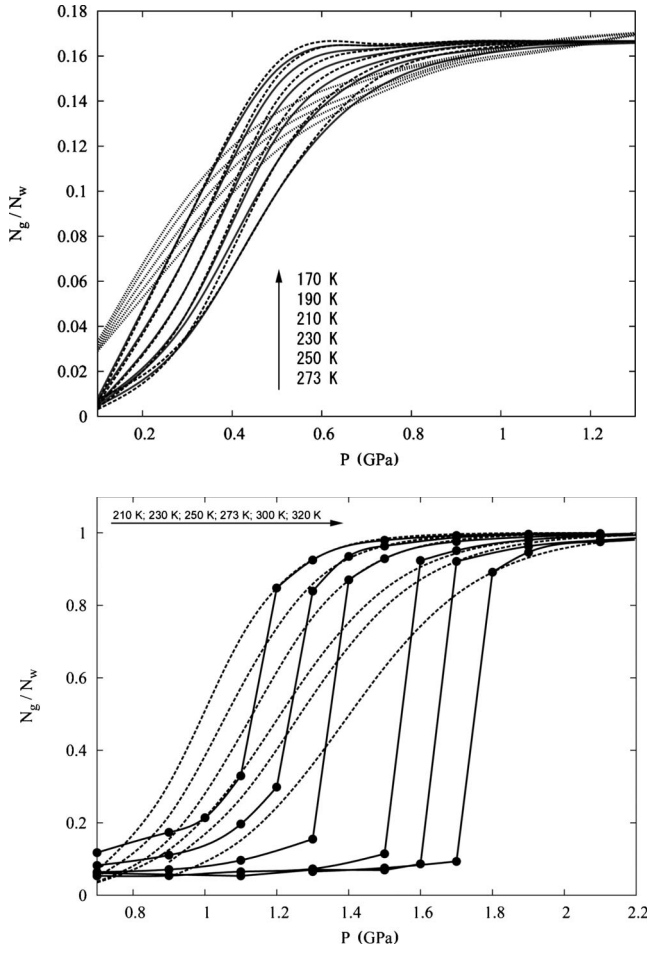

FIG. 3. Pressure and temperature dependence of hydrogen-to-water molar ratio in (a) C_1 and (b) C_2, obtained from GCMC simulation (solid line) and theoretical calculation based on vdWP theory (dashed line). The results from theoretical calculation based on one-dimensional partition function for C_1 is shown as dotted line (a).

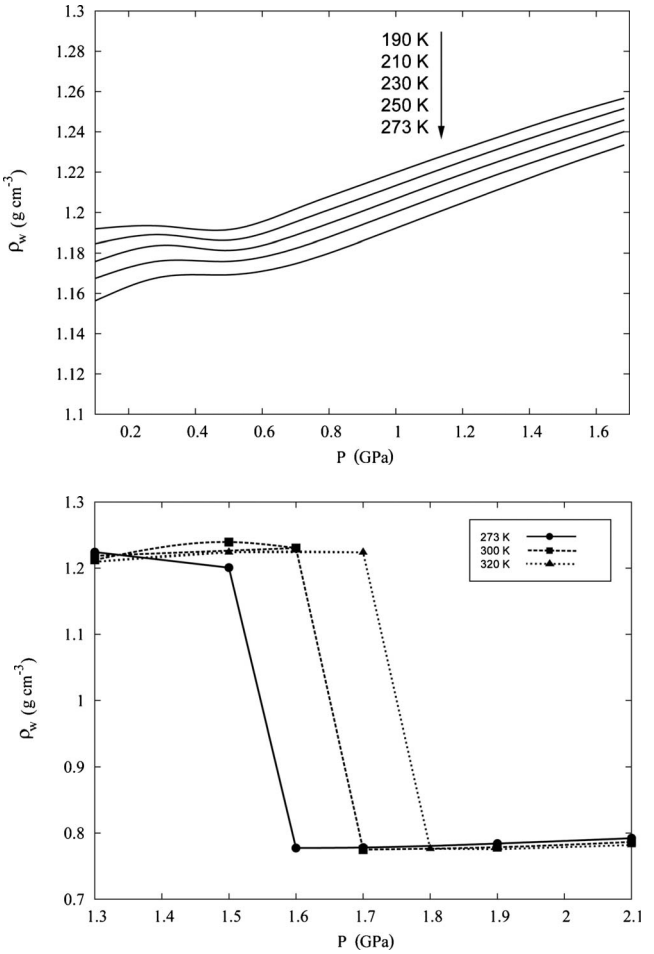

FIG. 4. Density of water in (a) C_1 and (b) C_2. A discontinuity in the density of C_2 suggests for a structure collapse of ice I_c lattice during decompression.

structural change may take place in ice I_c structure. The GC/NPT simulation shows that a high-density phase replaces the ice I_c structure at intermediate pressure region [Fig. 4(b)]. This can be attributed to the experimental evidence that another ice morphology is substituted for ice I_c at that pressure range[17] and the host lattice is stable only when almost all of the voids are filled with guest molecules. Here it is clear that ice I_c structure is no longer intact and is degraded to an amorphous structure when the ratio of hydrogen-to-water molecules drops below a certain value due to low pressure [Fig. 2(f)]. It is not surprising that hydrogen molecules stabilize the structure of ice I_c at high temperature and pressure in the same way as guest species stabilizes a clathrate hydrate. The maximum molar ratio of water hydrogen in C_2 is found to be 1:1. This value is also in agreement with the experiment.[10] The low ratio of hydrogen-to-water, observed when ice I_c is transformed to an amorphous ice, can be associated with the low but finite solubility of gas molecules in amorphous ice.[20]

B. Theoretical calculation of hydrogen occupancy inside ice I_c and ice II

The simulation results suggest that hydrogen molecules occupy a specific position in the voids of ice I_c [Fig. 2(d)]. Given the maximum molar ratio of hydrogen-to-water in C_2, it is possible to regard ice I_c of N_w water molecules as a host lattice having N_w virtual cages, each of which allows at most one hydrogen to occupy. This situation is then equivalent to the common clathrate hydrate whose stability can be estimated by vdWP theory.[21,22] The characteristic of this virtual cage should be examined prior to justify the treatment.

The potential-energy curve of a hydrogen molecule inside the virtual cage of ice I_c is calculated as a function of radial distance, r, from the originally stable position. The potential energy here is calculated from the interaction with all water molecules fixed to lattice sites. It is averaged over all molecular orientations and all cages. The resultant curve is given in Fig. 5 along with the minimum energy at a particular orientation at a given r. The potential-energy curve is rapidly increasing as the hydrogen molecule leaves its mechanically stable position. In contrast to the interaction energy of hydrogen molecules in a smaller cage of sII clathrate structure,[8] the interaction energy of hydrogen molecule in-

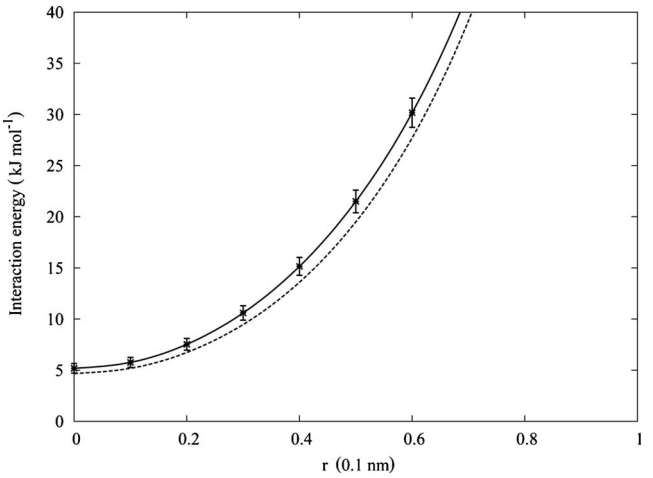

FIG. 5. Interaction energy curve of a hydrogen molecule with the surrounding water molecules in an interstitial space of ice I_c as a function of displacement from its stable position: averaged over all orientation (solid line); minimum energy (dashed line). The vertical bars show variance of interaction energy in other interstitial spaces of ice I_c.

side the interstitial space of ice I_c has a repulsive character even at its minimum due to the small size of the virtual cage. It is, yet, reasonable if we consider the high pressure needed to encage hydrogen molecule inside cubic ice. In addition, the repulsive interaction of the guest molecule is essential to maintain the mechanical stability of ice I_c framework. We carry out an MC NVT simulation of hydrogen fluid (at $T=273$ K) inside the cavity of ice I_c by fixing the water-lattice position, whose result indicates that the movement of hydrogen molecules is limited to about 0.4 nm from the original stable position. This limitation, indeed, does not directly correspond to the real situation, where hydrogen molecules can diffuse to a neighboring void when the thermal motion of water is considered.[23,24] However, the information about displacement limit is particularly useful in calculating the free energy of occupancy of hydrogen molecules inside ice I_c, where the maximum displacement from the center can be regarded as the size of each virtual cage. The vertical bars in Fig. 5 are the variance of interaction energy of hydrogen molecule in various cavities. The figure shows that all cavities are energetically equivalent; thus the free energy of occupancy is equal throughout.

The occupancy of hydrogen inside ice I_c can be estimated from a grand-canonical partition function. For the system with αN_w virtual cages, where α is equal to unity in the case of C_2, the partition function is given by

$$\Xi = \exp(-\beta A_w^0)(1+\exp[\beta(\mu_g - f_g)])^{\alpha N_w}, \tag{8}$$

where A_w^0 is the free energy of empty ice and f_g is the free energy of cage occupation. It is converted to the generalized partition function Υ assuming at most a single occupancy as

$$\Upsilon = \frac{1}{v_0}\int_0^\infty \Xi \exp(-\beta pV)dV, \tag{9}$$

where v_0 is the unit volume which is introduced to make the partition function dimensionless. The integral is actually replaced by the integrand $\Xi(V_m)\exp(-\beta pV_m)$ at equilibrium volume V_m where the integrand in Eq. (9) takes a maximum value. Then, it is reasonable that $\bar{f}_g$ is substituted for f_g at V_m and the partition function is approximated to

$$\Upsilon = \exp(-\beta G_w^0)(1+\exp[\beta(\mu_g - \bar{f}_g)])^{\alpha N_w}.$$

The mean number of hydrogen molecules is expressed as

$$\langle N_g \rangle = \frac{\partial \ln \Upsilon}{\partial(\beta\mu_g)} \tag{10}$$

and the cage occupancy, x, defined as $\langle N_g \rangle / \alpha N_w$ is given by

$$x = \frac{\exp[\beta(\mu_g - \bar{f}_g)]}{1+\exp[\beta(\mu_g - \bar{f}_g)]}, \tag{11}$$

where the free energy of cage occupancy $\bar{f}_g(f_g)$ is evaluated by integration of potential interaction between a linear symmetric molecule with the surrounding water molecules inside a cage at an equilibrium volume as

$$\exp(-\beta \bar{f}_g) = \left(\frac{2\pi m k_B T}{h^2}\right)^{3/2}\left(\frac{2\pi I k_B T}{h^2}\right) \times \int\int \exp[-\beta w(\mathbf{r},\Omega)]d\mathbf{r}d\Omega. \tag{12}$$

The estimated hydrogen occupancy inside ice I_c is plotted in Fig. 3(b) as dashed line. The theoretical prediction agrees well with that from the simulation in high-occupancy region but deviates significantly in low occupancy. The discrepancy is due to an assumption in theoretical calculation that the host structure (ice I_c in this case) is stable even in the absence of hydrogen at any pressures. The theoretical calculation necessarily leads to the partial occupancy and thus gives a smooth increase in hydrogen occupancy in ice I_c during compression since neither a possible instability of the host lattice nor the thermodynamic stability of this hydrate compound over ice VII (or ice II) is taken into consideration. The latter is considered in the estimation of a global phase diagram. In practical simulation (and also experiment), decompression gives rise to mechanical instability, which prevents the observation of C_2 at lower pressures. This is different from the thermodynamic stability that is determined by the chemical potentials and is argued below. The sudden collapse is, however, not found in the case of C_1, where the host structure is stable even in the absence of hydrogen molecules. Hence, a similar method can be applied to C_1 by dividing each cylindrical channel into cells, each of which contains only a single guest molecule. The obtained result, as given in Fig. 3(a) as dashed line, agrees well with the MC simulation over the entire pressure and temperature range studied. The successful predictions by this theoretical calculation indicate that an underlying mechanism in the accommodation of hydrogen is simple. It is determined by the free energy of cage occupation which is, in turn, dominated by the vacant space for a hydrogen molecule to be encaged, considering the weak interaction between water and hydrogen.

Another theoretical approach for calculating the occupancy of hydrogen inside ice II can be devised by considering that the hydrogen molecules arrange themselves in a quasi-one-dimensional manner in the cylindrical space of ice II [Fig. 2(c)]. The cylindrical space extends along the c axis (denoted as z direction here). The system then can be treated with one-dimensional partition function, which eventually leads to an estimation of the number density of hydrogen inside the cylindrical voids. The partition function can be exactly calculated if there is no interaction between molecules beyond nearest neighbors, that is, in our case, if each guest molecule is taken to interact with its nearest neighbors alone.[25,26] This approach may be reasonable since the potential for hydrogen pair, $\psi(z)$, is short ranged. Now let Π be a quantity with a dimension of force per unit length (a one-dimensional analogue of the pressure) and define a Laplace transform of $e^{-\beta\psi(z)}$ defined by

$$y = \int_0^\infty e^{-\beta\Pi z} e^{-\beta\psi(z)} dz. \tag{13}$$

Then the isobaric partition function Υ_{1D} for the one-dimensional gas is expressed as

$$\Upsilon_{1D}(\Pi,T) = e^{-N\beta\mu} = y^N e^{-N\beta f_1}/l_z^N, \tag{14}$$

where f_1 is the free energy of a single guest molecule occupying a cylindrical space of length l_z defined as

$$\exp(-\beta f_1) = \left(\frac{2\pi m k_B T}{h^2}\right)^{3/2}\left(\frac{2\pi I k_B T}{h^2}\right) \times \int_0^{l_z} dz \int dx \int dy \int d\mathbf{\Omega}\, \exp[-\beta w(\mathbf{r},\mathbf{\Omega})], \tag{15}$$

where $w(\mathbf{r},\mathbf{\Omega})$ is the interaction energy of a hydrogen molecule with all the water molecules. The relation between the chemical potential of hydrogen and Π is given by Eq. (13) or equivalently by

$$\mu = -k_B T \ln(y e^{-\beta f_1}/l_z) \tag{16}$$

and the number density ρ in the quasi-one-dimensional space (the number of molecules per unit length) is given by

$$\rho = -\left(\frac{\partial \ln y}{\partial \beta \Pi}\right)^{-1}. \tag{17}$$

The pressure dependences of the calculated occupancy at various temperatures with the nearest-neighbor assumption are shown in Fig. 3(a) (dotted line). The overall result, however, suggested that the treatment by vdWP theory is better suited for the present system which is characterized by high pressure and high density.

C. Compressibility of hydrogen hydrate of ice II and Ice I_c structure

The water lattice of ice VII consists of two interpenetrating, but not interconnecting, sublattices of ice I_c framework,[27] giving one of the densest ices as a result. Therefore, C_2 can alternatively be seen as ice VII where one of its water sublattice is replaced by hydrogen molecules. It is intriguing to evaluate the compressibility of C_2 and then compare it with that of the ice VII, thereby examining the consequence of the nonstoichiometry in C_2.

Let us begin with a system specified by (N_w, N_g, V, T) each indicating the number of water molecules, the number of guest molecules, the volume, and the temperature. In this paragraph on the thermodynamic properties, N_g is a mean value of the guest molecules in the clathrate hydrate and is identified with $\langle N_g \rangle$ in the remaining parts. The thermodynamic potential is the (Helmholtz) free energy, A. The infinitesimal change in the free energy of gas hydrate system is written as

$$dA = -pdV - SdT + \mu_w dN_w + \mu_g dN_g. \tag{18}$$

If μ_g, instead of N_g, is taken to be an independent variable, the thermodynamic potential for such a system is

$$\Phi = A - \mu_g N_g, \tag{19}$$

and the differential is

$$d\Phi = -pdV - SdT + \mu_w dN_w - N_g d\mu_g. \tag{20}$$

The system is now characterized by (V,T,N_w,μ_g). This condition meets exactly the vdWP theory. Here, we implicitly assume that the clathrate hydrate is in equilibrium with a guest fluid outside at T and μ_g. This kind of system is set up by surrounding the hydrate with a membrane permeable only to hydrogen molecule and thus preventing water molecule to leave the hydrate system. Then the pressure p_g of the fluid phase is, in general, different from the pressure p of the hydrate phase we are interested in: the gas hydrate is not in true equilibrium with the fluid of guest species. Consequently, the phase rule for the two-component system with two-phase equilibrium is not applied to the thermodynamic condition for the vdWP theory. Further, the constant-volume condition becomes unrealistic at high pressures where the change in V cannot be neglected. These limitations in the original vdWP theory are circumvented by introducing another thermodynamic potential

$$\Psi = \Phi + pV. \tag{21}$$

We obtain

$$d\Psi = Vdp - SdT - N_g d\mu_g + \mu_w dN_w, \tag{22}$$

which implies this thermodynamic potential is a function of p, T, N_w, and μ_g. Integrating Eq. (22) gives

$$\Psi = \mu_w N_w. \tag{23}$$

We further impose an experimentally accessible condition that the clathrate hydrate is in equilibrium with a fluid mixture of hydrogen and water. This is realized by requiring that the chemical potentials of water and hydrogen in the fluid phase are equal to those in the clathrate and the pressure in the fluid is equal to p in Eq. (21). Then, the term $d\mu_g$ in Eq. (22) is replaced in terms of dp and dT from Gibbs-Duhem equations as

$$d\mu_g = \left(\frac{1-a}{1-ab}\right)v_g dp - \left(\frac{1-ac}{1-ab}\right)s_g dT, \tag{24}$$

where v_g is the volume per molecule and s_g is the entropy per molecule in the fluid phase and a, b, and c are defined using number density $\rho=N/V$ and entropy density $\eta=S/V$ for each phase and each component as

$$a = \rho_w^{(\text{fluid})}/\rho_w^{(\text{hydrate})}, \quad b = \rho_g^{(\text{hydrate})}/\rho_g^{(\text{fluid})},$$
$$c = \eta^{(\text{hydrate})}/\eta^{(\text{fluid})}. \tag{25}$$

It is now transparent that the potential Ψ is a function of p, T, and N_w. In the limit of $\rho_w \approx 0$ or $\rho_w \ll \rho_g$, $d\mu_g$ in Eq. (24) is approximated to $v_g dp + s_g dT$. Therefore, we are left with

$$d\Psi = (V - V_g)dp - (S - S_g)dT + \mu_w dN_w, \tag{26}$$

where $V_g=N_g v_g$ and $S_g=N_g s_g$. Note that $V-V_g$ in Eq. (26) formally refers to the volume of water, which can be either positive or negative. The chosen thermodynamic potential corresponds to the generalized isobaric partition function Υ as defined in Eq. (9) while Eq. (26) suggests that its differentiation leads to the properties of water lattice in hydrate system.

The volume and its derivatives can be obtained by the theoretical method as well as GC/NPT MC simulation. The partition function which corresponds to the thermodynamic potential in Eq. (26) can be written as

$$-k_B T \ln \Upsilon = G_w^0 - \alpha k_B T N_w \ln\{1 + \exp[\beta(\mu_g - \bar{f})]\}. \tag{27}$$

Its differentiation with respect to the pressure then gives the volume of water in hydrate system

$$V_w = V_w^0 + \alpha N_w x\left(\frac{\partial \bar{f}}{\partial p} - \frac{\partial \mu_g}{\partial p}\right) \tag{28}$$

with $\alpha N_w x=\langle N_g \rangle$ and $(\partial \mu_g/\partial p)=v_g$. The volume of the system is given by rearranging Eq. (28) so that

$$V = V_w^0 + \alpha N_w x \frac{\partial \bar{f}}{\partial p}. \tag{29}$$

By the definition, the compressibility is

$$\kappa_T = -\frac{1}{V}\frac{\partial V}{\partial p} \tag{30}$$

and with $V_w^0=N_w v_w^0$, thus it is given as

$$\kappa_T = -\frac{\frac{\partial v_w^0}{\partial p} + \alpha \frac{\partial x}{\partial p}\frac{\partial \bar{f}}{\partial p} + \alpha x \frac{\partial^2 \bar{f}}{\partial p^2}}{v_w^0 + \alpha x \frac{\partial \bar{f}}{\partial p}}. \tag{31}$$

An alternative method to evaluate the compressibility from theoretical approach is given by considering a fact that the integrand of the partition function in Eq. (9) is maximum at equilibrium so that

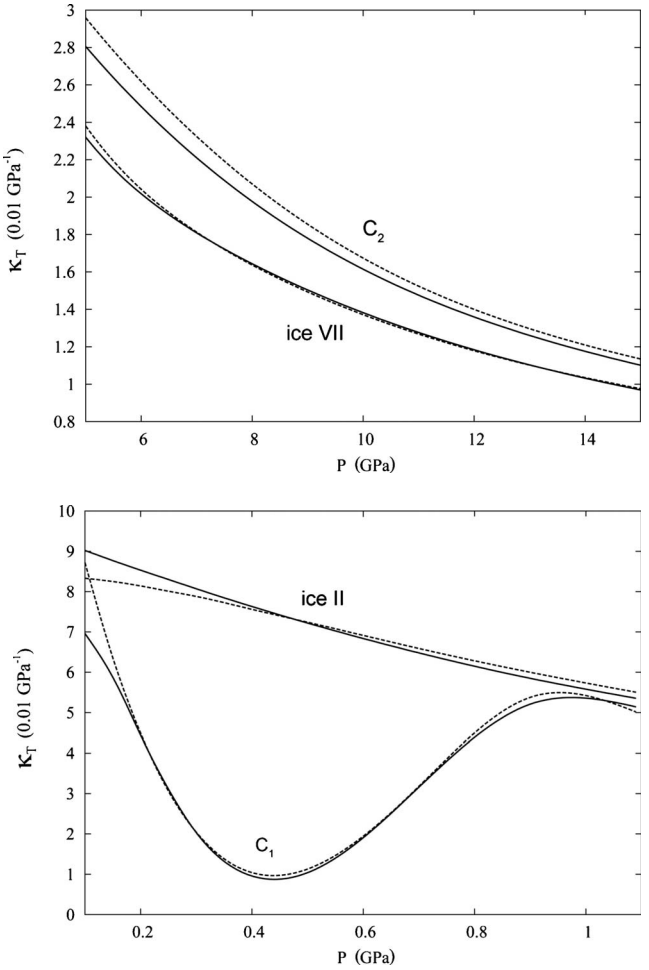

FIG. 6. Isothermal compressibility of (a) C_2 and ice VII, (b) C_1 and ice II, obtained from free-energy calculation (solid line) and GCMC simulation (dashed line).

$$-k_B T \frac{\partial \ln \Xi \exp(-\beta pV)}{\partial V} = 0, \tag{32}$$

$$p = -\frac{\partial a_w^0}{\partial v} - \alpha \frac{\partial f}{\partial v} x, \tag{33}$$

and the inverse of compressibility, also known as bulk modulus, can be written as

$$\kappa_T^{-1} = -\frac{\partial p}{\partial \ln V} = v\frac{\partial^2 a_w^0}{\partial v^2} + \alpha v \frac{\partial^2 f}{\partial v^2} x + \alpha v \frac{\partial f}{\partial v}\frac{\partial x}{\partial v}. \tag{34}$$

The isothermal compressibility of C_2 and ice VII in a pressure region where both species are thermodynamically stable is shown in Fig. 6(a). The compressibility from the free-energy calculation is compared with that from GCMC simulation, which results in nearly complete agreement. In the pressure range studied, the compressibility of ice VII is found to be lower than C_2. This can be caused either by the ability of water molecules to build a firm hydrogen-bonded structure and/or simply because the size of water molecule is larger than hydrogen. In addition, the obtained p-V-T data and bulk modulus of ice VII from simulation and theoretical

calculation are close to those obtained from an experimental work with diamond-anvil cell at the same pressure range of gigapascal order.[28] Another experimental work reported that the decrease in C_2 volume with the increase in pressure is greater compared to the case of ice VII, which suggested that the compressibility of C_2 is higher than ice VII.[29]

The compressibility of ice II and C_1 can also be evaluated in a similar way. Since C_1 structure remains stable in partial hydrogen occupancy, which is different from the case of C_2, the evaluation can be done in a pressure region where hydrogen gradually fills the cylindrical spaces in C_1. The compressibility of C_1 and pure ice II, obtained from free-energy calculation and GCMC simulation, is shown in Fig. 6(b). At pressure region where hydrogen molecules start to fill the empty space of ice II, a significant deviation from the compressibility line of empty ice II is observed. This large change in compressibility can be understood better by examining the change in the C_1 volume when hydrogen start to occupy the cylindrical spaces in ice II as shown in Fig. 4(a). The deviation of C_1 volume from the pure ice II is led by two opposite factors in the course of compression; a high chemical potential increases the number of hydrogen molecules in ice cavities, which, in turn, expands the size of hexagonal rings and increases the volume, but it is partially cancelled by the simple hydrostatic pressure which reduces ice volume. This gives rise to a complicated pressure dependence of the volume. The deviation, in turn, yields the large change in compressibility of C_1 during partial occupancy. The second term on the right-hand side in Eq. (34) is found to give a major contribution to the magnitude of compressibility. This term is also immensely determined by the magnitude of the occupancy and vanishes in the absence of hydrogen molecules. Such complicated pressure dependence is not observed in C_2 since the lattice structure is unstable under partial occupancy of hydrogen.

D. Thermodynamic stability of C_1 and C_2

The thermodynamic stability of C_1 and C_2 can be quantified in terms of the chemical potential, which eventually enables us to predict the phase boundaries between them. The chemical potential of water in C_1 and C_2 is calculated as

$$-\frac{\partial \ln \Upsilon}{\partial \beta N_{\mathrm{w}}} = \mu_c = \mu_c^0 + \alpha k_{\mathrm{B}} T \ln(1-x), \tag{35}$$

where

$$\mu_c^0 = (A_{\mathrm{w}}^0 + pV)/N_{\mathrm{w}} \tag{36}$$

is the chemical potential of the empty ice. The Helmholtz free energy of ice containing no hydrogen molecule, A_{w}^0, is approximated by the sum of the potential energy at its minimum structure, U_{q}, the harmonic free energy, F_{h}, and the residual entropy term, S_c (if any), as

$$A(T,V) = U_{\mathrm{q}}(V) + F_{\mathrm{h}}(T,V) - TS_c \tag{37}$$

with

$$F_{\mathrm{h}}(T,V) = k_{\mathrm{B}} T \sum_i \ln\left(\frac{h\nu_i}{k_{\mathrm{B}} T}\right), \tag{38}$$

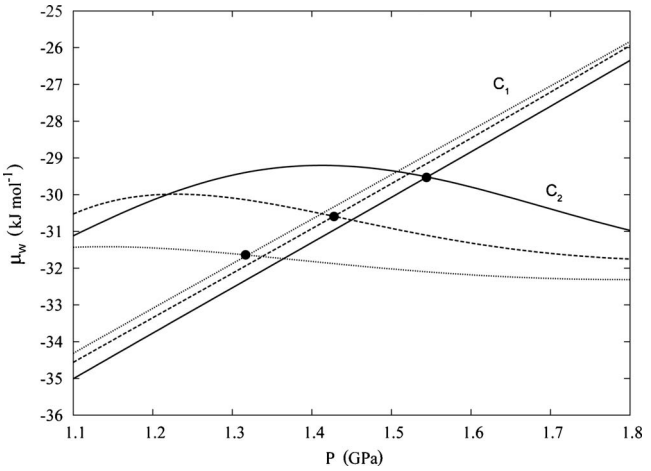

FIG. 7. Chemical potential of water in C_1 (linear) and C_2 (curve) at $T=273$ K (solid line), 250 K (dashed line), and 230 K (dotted line). The chemical-potential shifts suggest a structure transition from C_1 to C_2 as the compression proceeds.

$$S_c = N_{\mathrm{w}} k_{\mathrm{B}} \ln(3/2). \tag{39}$$

The harmonic free energy of water is calculated from normal-mode analysis.[30–33] Here the free energy arising from anharmonic contribution is neglected because only the difference in the anharmonic free energy between empty ice and filled ices is required in the thermodynamic stability as discussed below and it is much smaller than the other term.[34]

Since the occupancy in C_2 is approximately unity at high pressure and the water-lattice vibrations are possibly shifted to higher frequencies, the harmonic free energy should be evaluated in the presence of hydrogen, and thus the chemical potential is replaced by the corresponding μ_{I_c}' which may include the modulation of intermolecular vibrational frequency by including "ghost" hydrogen.[35] Equation (35) is rewritten in a more convenient form

$$\mu_c = \mu_c' + \alpha(f_{\mathrm{g}} - \mu_{\mathrm{g}} + k_{\mathrm{B}} T \ln x). \tag{40}$$

This serves to suppressing statistical errors in evaluating the thermodynamic stability from GC/NPT simulations which may arise from logarithm term. More importantly, change to the new standard state is an essential manipulation in the case of C_2 since otherwise ice I_c collapses at high pressure.

The calculated chemical potential as a function of pressure and temperature for C_1 and C_2 are plotted in Fig. 7. At $T=273$ K and $p \leq 1.5$ GPa, C_1 structure has lower chemical potential which explains its existence in preference to C_2 while C_2 has higher chemical potential when the hydrogen occupancy in its voids is low. As the pressure increases and the hydrogen molecules start to occupy the voids inside ice I_c, the chemical potential of C_2 becomes lower than C_1. In other word, C_2 structure is more favorable than C_1 at high pressure ($P \geq 1.6$ GPa). This is also in agreement with the experimental fact that C_2 structure is observed at higher pressure region and C_1 structure at lower pressure region.

E. Phase diagram of C_1 and C_2

The C_1 and C_2 phases occupy neighboring regions in the phase diagram but the phase boundaries are not fully established especially in composition axis. We show that a global phase diagram is obtained from evaluation of the chemical potentials for water and/or hydrogen. From now on, α denotes exclusively the cage-to-water ratio for C_1 while that for C_2 (=1) is not shown explicitly. The triple-point pressure p_0 for the $C_1+C_2+H_2$ coexistence (which is a line in the complete phase diagram including T) is obtained from condition that the chemical potentials of water are equal in C_1 and C_2 phases as

$$\mu_{C1} = \mu_{C2} \quad \text{and} \quad \mu_g = \mu_g^0(T,p),$$

where $\mu_{C1}=\mu_{II}^0+\alpha k_B T \ln(1-x_1)$ and $\mu_{C2}=\mu_{I_c}'+k_B T \ln(1-x_2)$ with

$$x_1 = \frac{\exp[\beta(\mu_g - f_{g1})]}{1+\exp[\beta(\mu_g - f_{g1})]} \quad \text{and} \quad x_2 = \frac{\exp[\beta(\mu_g - f_{g2})]}{1+\exp[\beta(\mu_g - f_{g2})]}. \tag{41}$$

Here μ_g^0 stands for the chemical potential of pure hydrogen fluid and suffices 1 and 2 refer to C_1 and C_2, respectively. The above condition determines the pressure p_0 and the occupancies x_1^0 and x_2^0 at the triple point.

The phase boundary between the C_2 phase and the C_2+H_2 coexistence is obtained from the occupancy in C_2 at a given T, which is

$$x_2 = \frac{\exp[\beta(\mu_g - f_{g2})]}{1+\exp[\beta(\mu_g - f_{g2})]} \quad \text{with} \quad \mu_g = \mu_g^0(T,P).$$

The phase boundary between the C_1 phase and the C_1+H_2 coexistence can also be determined in similar manner.

Since C_2 is stable when hydrogen-water molecular ratio is greater than a certain value, then there is a region in phase diagram where only C_2 is stable (single phase). Consequently, another boundary should appear at the lower mole fraction; that is between the C_2 phase and the C_1+C_2 coexistence. At this boundary, hydrogen in C_2 is supposed to be in equilibrium with hydrogen in C_1 at the same T, p but not necessarily in equilibrium with pure hydrogen fluid. For this reason, it is determined by removing the unknown μ_g, where

$$\mu_g = f_1 + k_B T \ln\left(\frac{x_1}{1-x_1}\right) = f_2 + k_B T \ln\left(\frac{x_2}{1-x_2}\right), \tag{42}$$

$$\Delta f = f_2 - f_1 = k_B T \ln\left(\frac{x_1(1-x_2)}{x_2(1-x_1)}\right). \tag{43}$$

It is reasonable to assume that most of the cavities are occupied in both hydrates at a high pressure above p_0, thus

$$\Delta f \approx k_B T \ln\frac{(1-x_2)}{(1-x_1)}. \tag{44}$$

We further apply a simple approximation that Δf is independent of the pressure. Now let us define $\Delta\mu$ as

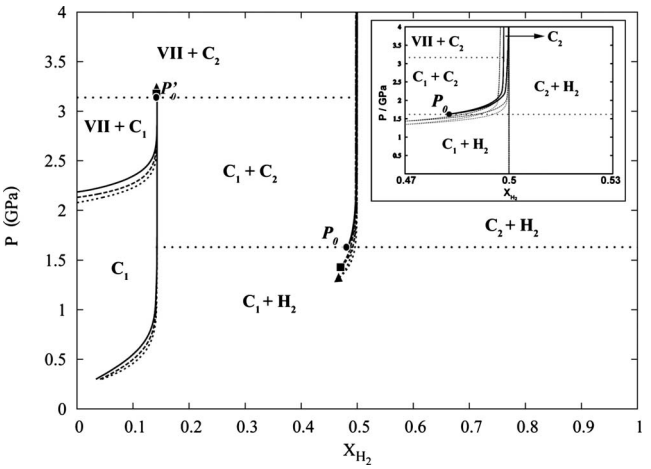

FIG. 8. Phase diagram of C_1 and C_2 on p-x_H plane at $T=273$ K (solid line and circle point), 250 K (dashed line and square point), and 230 K (dotted line and triangle point). The horizontal line shows the triple point of $C_1+C_2+H_2$ coexistence and C_2+C_1+VII coexistence. They also marked the phase boundary between C_1, C_1+C_2, and C_2 on p-T plane.

$$\Delta\mu = \mu_{I_c}' - \mu_{II} = \alpha k_B T \ln(1-x_1) - k_B T \ln(1-x_2). \tag{45}$$

Since $\Delta\mu=\Delta a+p\Delta v$ with $\Delta v=v_2-v_1$ at fixed p for single component, combined with Eq. (44), the occupancy x_2 is obtained as

$$D \exp\left\{-\frac{\beta(\Delta a + p\Delta v)}{1-\alpha}\right\} = 1 - x_2 \tag{46}$$

with $D=\exp[\alpha\Delta f/k_B T(\alpha-1)]$, which leads further to

$$x_2 - x_2^0 = (1-x_2^0)\left(1-\exp\left\{-\frac{\beta\Delta p\Delta v}{1-\alpha}\right\}\right) \tag{47}$$

with $\Delta p=p-p_0$. Additionally, x_1 in this equilibrium can be obtained from Eq. (44).

Since C_1 is stable even in the case of partial occupancy, the region where only C_1 is stable can be expected to be wider than C_2. The phase boundary between C_1+ice VII and C_1 phase, as well as the triple point pressure p_0' for the C_1+C_2+ice VII coexistence, can be predicted according to the following condition:

$$\mu_{VII} = \mu_{C1} = \mu_{II} + \alpha k_B T \ln(1-x_1), \tag{48}$$

$$x_1 = 1 - \exp\left\{\frac{\Delta\mu}{\alpha k_B T}\right\} \tag{49}$$

with $\Delta\mu=\mu_{VII}-\mu_{II}$.

The global phase diagram is shown in Fig. 8. In the p-x_H (mole fraction of H_2) plane where T is fixed, a one-phase state (C_1 or C_2) and a two-phase equilibrium state (ice VII $+C_1$, VII$+C_2$, C_1+C_2, C_1+H_2, or C_2+H_2) form finite areas while a three-phase equilibrium state or a triple point (ice VII$+C_1+C_2$ or $C_1+C_2+H_2$) appears as a line, where H_2 stands for the hydrogen-fluid phase. When $p<p_0$, for any value of x_H, the chemical potential of water in C_2 is higher than that in C_1, and thus C_2 is not stable in this region. When

$p > p_0$, the C_2 phase is in equilibrium with C_1 or with ice VII for $x_H < 0.5$ while it is in equilibrium with a hydrogen fluid for $x_H > 0.5$. In between, there is a narrow region (appeared to be a line in Fig. 8 but it is actually a region as shown in the inset), where C_2 is the only stable phase. This region becomes wider as the temperature decreases, hence signifying higher stability of cubic ice structure at lower temperature. Here it is shown that the existence of a particular hydrogen hydrate phase can be regulated by varying its chemical composition. The phase boundaries predicted from theoretical calculation are in good agreement with the experimental observation, that is, C_2 becomes more stable than C_1 at high pressure range, and it coexists with the C_1 phase at middle pressure ranges.[10] Furthermore, p_0 is shown to have a positive slope in p-T plane while p_0' has a negative slope, which is also in agreement with experimental observation. It should also be noted that the pressure where ice I_c structure collapses in Fig. 3(b) is close to the triple-point pressure p_0.

IV. CONCLUDING REMARKS

In summary, we propose a theoretical method with the extension of the vdWP theory to estimate the thermodynamic stability of ice II and ice I_c filled with hydrogen, which are called C_1 and C_2, via occupancies calculation. The calculated result is then compared with that from GC/NPT MC simulations. The C_1 phase is stable under partial occupancy and gradually encages hydrogen with increasing pressure while C_2 is stable only when most of its voids are occupied by hydrogen molecules. The maximum molar ratio of hydrogen-water is found to be 1:6 and 1:1 for C_1 and C_2, respectively. There is no phase transition observed during the change in hydrogen occupancy in C_1 but a substitution of ice I_c morphology in C_2 compounds is observed when the molar ratio of hydrogen-water drops below certain value, depending on pressure and temperature. For this reason, partial occupancy of hydrogen molecule inside ice I_c is unlikely to happen since the ice I_c structure is unstable and collapses in the absence of hydrogen molecules inside its voids under high pressure and temperature. The existence of hydrogen molecules inside the vacant spaces of ice II and ice I_c enhances the stability of ice structure and shift the phase boundary of both ices to higher pressure and temperature region. We propose an appropriate ensemble, a partition function, and the relevant thermodynamic potential to characterize the hydrogen hydrates. It is found that the theoretical calculation based on a modified vdWP theory for the present systems successfully reproduces the hydrogen occupancies obtained by direct MC simulations. This allows us to evaluate the stability of various forms of filled ices without any fitting parameters or inputs from experiments. The compressibility of C_1 and C_2 obtained from derivation of a relevant partition function is found to reproduce the compressibility obtained by MC simulation. The results give a description on two opposing factors in C_1 compression and a comparison between the compressibility of C_2 and its closely related ice VII. Phase boundaries in the pressure-composition phase diagram at various temperatures are estimated from the chemical-potential calculation of water and are also found to be consistent with experimental observations in p-T plane,[10] that is, C_1 is replaced by C_2 as the compression proceeds to higher pressure, p_0 has positive slope and p_0' has negative slope. Furthermore, the region where C_2 is the only stable phase is getting wider with the decrease in temperature, signifying higher stability of ice I_c at lower temperature. From the obtained phase diagram in p-x_H, it is evident that a certain hydrogen hydrate structure, in single form or mixtures, can be obtained by controlling the composition of water and hydrogen. The phase diagram will be an important guideline for experiments to obtain a certain type of hydrogen hydrate structure, either as a single phase or coexisting phases.

ACKNOWLEDGMENTS

This work was supported by grant-in-aid from JSPS and MEXT and the Next Generation Super Computing Project, Nanoscience Program, MEXT, Japan, and also Okayama Foundation for Science and Technology. The authors are grateful to H. Itoh for providing the ice II structure.

[1] L. Schlapbach and A. Zuttel, Nature (London) **414**, 353 (2001).
[2] V. V. Struzhkin, B. Militzer, W. L. Mao, H. Mao, and R. J. Hemley, Chem. Rev. **107**, 4133 (2007).
[3] H. Lee, J. W. Lee, D. Y. Kim, J. Park, Y. T. Seo, H. Zeng, I. L. Moudrakovski, C. I. Ratcliffe, and J. A. Ripmeester, Nature (London) **434**, 743 (2005).
[4] Y. H. Hu and E. Ruckenstein, Angew. Chem., Int. Ed. **45**, 2011 (2006).
[5] W. L. Mao and H. Mao, Proc. Natl. Acad. Sci. U.S.A. **101**, 708 (2004).
[6] K. Lokshin, Y. Zhao, D. He, W. L. Mao, H. Mao, R. J. Hemley, M. V. Lobanov, and M. Greenblatt, Phys. Rev. Lett. **93**, 125503 (2004).
[7] T. A. Strobel, C. A. Koh, and E. D. Sloan, J. Phys. Chem. B **112**, 1885 (2008).
[8] K. Katsumasa, K. Koga, and H. Tanaka, J. Chem. Phys. **127**, 044509 (2007).
[9] N. I. Papadimitriou, I. N. Tsimpanogiannis, C. J. Peters, A. Th. Papioannou, and A. K. Stubos, J. Phys. Chem. B **112**, 14206 (2008).
[10] W. L. Vos, L. W. Finger, R. J. Hemley, and H. K. Mao, Phys. Rev. Lett. **71**, 3150 (1993).
[11] D. Eisenberg and W. Kauzmann, *The Structure and Properties of Water* (Oxford University Press, London, 1969).
[12] D. Londono, W. F. Kuhs, and J. L. Finney, Nature (London) **332**, 141 (1988).
[13] Yu. A. Dyadin, É. G. Larionov, E. Ya. Aladko, A. Yu. Manakov, F. V. Zhurko, T. V. Mikina, V. Yu. Komarov, and E. V. Grachev, J. Struct. Chem. **40**, 790 (1999).
[14] L. Hakim, K. Koga, and H. Tanaka, Phys. Rev. Lett. **104**,

115701 (2010).
[15] I. F. Silvera and V. Goldman, J. Chem. Phys. **69**, 4209 (1978).
[16] W. L. Jorgensen, J. Chandrasekhar, J. D. Madura, R. W. Impey, and M. L. Klein, J. Chem. Phys. **79**, 926 (1983).
[17] Y. Koyama, H. Tanaka, G. T. Gao, and X. C. Zeng, J. Chem. Phys. **121**, 7926 (2004).
[18] I. Ohmine, H. Tanaka, and P. G. Wolynes, J. Chem. Phys. **89**, 5852 (1988).
[19] J. D. Bernal and R. H. Fowler, J. Chem. Phys. **1**, 515 (1933).
[20] A. Bar-Nun, J. Dror, E. Kochavi, and D. Laufer, Phys. Rev. B **35**, 2427 (1987).
[21] J. H. van der Waals and J. C. Platteeuw, Adv. Chem. Phys. **2**, 1 (1959).
[22] E. D. Sloan and C. A. Koh, *Clathrate Hydrates of Natural Gases*, 3rd ed. (CRC Press, Boca Caton, FL, 2008).
[23] T. Okuchi, M. Takigawa, J. Shu, H. K. Mao, R. J. Hemley, and T. Yagi, Phys. Rev. B **75**, 144104 (2007).
[24] T. Ikeda-Fukazawa, S. Horikawa, T. Hondoh, and K. Kawamura, J. Chem. Phys. **117**, 3886 (2002).
[25] M. Bishop and M. A. Boonstra, Am. J. Phys. **51**, 564 (1983).
[26] H. Tanaka and K. Koga, J. Chem. Phys. **123**, 094706 (2005).
[27] B. Kamb and B. L. Davis, Proc. Natl. Acad. Sci. U.S.A. **52**, 1433 (1964).
[28] Y. Fei, H. Mao, and R. J. Hemley, J. Chem. Phys. **99**, 5369 (1993).
[29] S. Machida, H. Hirai, T. Kawamura, Y. Yamamoto, and T. Yagi, J. Chem. Phys. **129**, 224505 (2008).
[30] A. Pohorille, L. R. Pratt, R. A. LaViolette, M. A. Wilson, and R. D. MacElroy, J. Chem. Phys. **87**, 6070 (1987).
[31] H. Tanaka and K. Kiyohara, J. Chem. Phys. **98**, 4098 (1993).
[32] H. Tanaka and K. Kiyohara, J. Chem. Phys. **98**, 8110 (1993).
[33] H. Tanaka, J. Chem. Phys. **101**, 10833 (1994).
[34] T. Nakayama, K. Koga, and H. Tanaka, J. Chem. Phys. **131**, 214506 (2009).
[35] The Hessian matrix of the whole system is given by

$$\mathbf{V} = \begin{pmatrix} \mathbf{V}_{ww} & \mathbf{V}_{gw} \\ \mathbf{V}_{wg} & \mathbf{V}_{gg} \end{pmatrix},$$

where V_{ij} indicates a submatrix associated with i and j species. In the presence of guest hydrogen, V_{ww} differs that in empty ice without guest hydrogen. The difference arises from the interactions between guest and host differentiated twice by the coordinates of water molecules.